

## Chapter 2

# A Spatio-Temporal Analysis Approach for Short-Term Forecast of Wind Farm Generation

In this chapter, short-term forecast of wind farm generation is investigated by applying spatio-temporal analysis to extensive measurement data collected from a large wind farm where multiple classes of wind turbines are installed. Specifically, using the data of the wind turbines' power outputs recorded across two consecutive years, graph-learning based spatio-temporal analysis is carried out to characterize the statistical distribution and quantify the level crossing rate of the wind farm's aggregate power output. Built on these characterizations, finite-state Markov chains are constructed for each epoch of 3 h and for each individual month, which accounts for the diurnal non-stationarity and the seasonality of wind farm generation. Short-term distributional forecasts and a point forecast are then derived by using the Markov chains and ramp trend information. The distributional forecast can be utilized to study stochastic unit commitment and economic dispatch problems via a Markovian approach. The developed Markov-chain-based distributional forecasts are compared with existing approaches based on high-order autoregressive models and Markov chains by uniform quantization, and the devised point forecasts are compared with persistence forecasts and high-order autoregressive model-based point forecasts.

## 2.1 Introduction

A critical aspect in meeting the renewable portfolio standard (RPS) adopted by many states in the U.S. includes the integration of renewable energy sources, such as wind and solar [4]. Given the fact that the power outputs of wind turbines are highly dependent on wind speed, the power generation of a wind farm varies across multiple timescales of power system planning and operations. With increasing penetration into bulk power systems, wind generation has posed significant challenges for reliable system operations, because of its high variability and non-dispatchability [5]. Specifically, one key complication arises in terms of committing and dispatching conventional generation resources, when the short-term forecast of wind farm generation is not accurate. Currently, wind generation forecast for an individual wind farm typically has an error of 15–20 % [13], in sharp contrast to the case of load

forecast. When the actual wind generation is above the forecasted value, i.e., more conventional generation capacity has been committed than needed, it could result in less efficient set points for thermal units. In some cases, wind generation may need to be curtailed [6]. On the flip side of the coin, when the actual wind generation is less than the forecasted value, costly ancillary services and fast acting reserves have to be called upon. Therefore, it is imperative to develop accurate forecast approaches for wind farm generation.

State-of-the-art short-term wind power forecast approaches include time-series models (e.g., autoregressive models [24], Kalman filtering [3]), Markov chains [2, 21], and data mining [11, 27]. A comprehensive literature review on wind power forecast can be found in [7] and [16]. Time-series models and data mining-based regression models, while being able to provide continuous-value wind power forecast, could suffer from high computational complexity. Compared to other forecast models, finite-state Markov chains strike a good balance between complexity and modeling accuracy. In particular, the transition probability matrix of Markov chains, which is used to provide distributional forecasts and point forecasts, can be learned from historical data (e.g., by using the maximum likelihood estimation technique [21]); when new data points are available online, it is also easy to update the transition probability matrix. It is worth noting that one of state-of-the-art forecasting approaches is to utilize empirical distributions and the rich statistical information extracted from historical data (see [20, 23] and the references therein). Generally, empirical distribution of wind power data is non-Gaussian [12]. In [22], the logit transform is carried out as preprocessing, so that such a bounded time series can be studied by using autoregressive models in a Gaussian framework. In this paper, finite-state Markov chains are utilized to model the bounded wind power time series with a general probability distribution. It is worth noting that finite-state Markov chains inherently have bounded support, and the stationary distribution of a Markov chain can be general. Despite the appealing features of Markov chains, there is no existing studies to systematically design the state space of Markov chains for wind power. The proposed approach in this chapter addresses this issue by developing a general spatio-temporal analysis framework.

In this chapter, Markov-chain-based stochastic models for wind farm generation are developed for different seasons and for different epochs of the day across the whole year. From these Markov-chain-based stochastic models, short-term distributional forecasts and point forecasts of wind farm generation are obtained. The information used for forecasts includes both historical data and real-time data (the present wind farm generation). With a forecasting lead time of 10 min (or larger), these Markov-chain-based forecasts could be utilized for a variety of power system operation functions.

One key observation of this study is the wind farm spatial dynamics, i.e., *the power outputs of wind turbines within the same wind farm can be quite different, even if the wind turbines are of the same class and physically located close to each other*. The disparity in the power outputs of wind turbines may be due to the wake effect of wind speed, diverse terrain conditions, or other environmental effects. Motivated by this observation, graph-learning based spatial analysis is carried out to quantify

the statistical distribution of *wind farm generation*, with rigorous characterization of wind farm spatial dynamics. Then, time series analysis is applied to quantify the level crossing rate (LCR) of the wind farm's aggregate power output. Finite-state Markov chains are then constructed, with the state space and transition matrix designed to capture both the spatial and temporal dynamics of the wind farm's aggregate power output. Based on [17], the distributional forecasts and the point forecasts of wind farm generation are provided by using the Markov chains and ramp trend information.

In this chapter, another finding of independent interest is that the tail probability of wind farm's aggregate power output exhibits a "power-law" decay with an exponential cut-off, where the power-law part has a much heavier tail than the Gaussian distribution. This indicates that one cannot simply apply the central limit theorem (CLT) to characterize the aggregate power output, because of the strong correlation across the power outputs of wind turbines within a wind farm.

The main contents of this chapter are summarized below:

- A general spatio-temporal analysis framework is developed, in which the spatial and temporal dynamics of wind farm generation are characterized by analytically quantifying the statistical distribution and the LCR.
- Built on the results of spatio-temporal analysis, a systematic approach for designing the state space of the Markov chain is introduced.

The rest of the chapter is organized as follows. A few critical observations from the measurement data are first discussed in Sect. 2.2. Spatio-temporal analysis and the design of Markov chains are presented in Sect. 2.3. Sect. 2.4 discusses the proposed Markov-chain-based forecast approach and numerical examples. A summary of the chapter is provided in Sect. 2.5. The main notation used in the chapter is summarized in Table 2.1.

## 2.2 Available Data and Key Observations

In this chapter, spatio-temporal analysis is carried out for a large wind farm with a rated capacity of  $P_{ag}^{\max}=300.5$  MW. There are  $M = 2$  classes of wind turbines in this wind farm, with  $N_1 = 53$  and  $N_2 = 221$ , respectively. The power curves of the two turbine classes are provided in Fig. 2.1. For each class  $C_m$ , a meteorological tower (MET)  $H_m$  is deployed and co-located with a wind turbine, denoted by  $r_m$ . The power outputs of all wind turbines and the wind speeds measured at all METs are recorded every 10 min for the years 2009 and 2010. From the measurement data, several key observations can be made as follows.

### 2.2.1 Spatial Dynamics of Wind Farm

A critical observation from the measurement data is that the power outputs of wind turbines within the wind farm can be quite different. Figure 2.2 illustrates the power

**Table 2.1** Summary of the main notation

Notation	Definition
$t$	Time index of measurement data
$m$	Index of wind turbine class and the corresponding meteorological tower (MET)
$M$	Number of wind turbine classes within the wind farm
$C_m$	Wind turbine class $m$
$N_t$	Number of measurement data
$N_m$	Number of wind turbines in $C_m$
$H_m$	MET for $C_m$
$r_m$	Wind turbine co-located with $H_m$ in $C_m$
$W_m(t)$	Wind speed measured at $H_m$
$P_i(t)$	Power output of wind turbine $i$
$U_m(\cdot)$	Power curve of $C_m$ , which maps $W_m(t)$ to $P_i(t)$ , $\forall i \in C_m$
$P_{ag,m}(t)$	Aggregate power output of $C_m$
$P_{ag}(t)$	Aggregate power output of the wind farm
$P_{ag}^{\max}$	Rated capacity of the wind farm
$\bar{m}$	Index of the reference MET
$d_m(i)$	“distance” from node $i$ to the root of the minimal spanning tree of $C_m$
$\alpha_m$	linear regression coefficient for the parent-child turbine pairs of $C_m$
$\beta_m$	Linear regression coefficient for $W_m(t)$ as an affine function of $W_{\bar{m}}(t)$
$G_{pw}(\cdot)$	“power curve” of the wind farm, which maps $W_{\bar{m}}(t)$ to $P_{ag}(t)$
$\Gamma$	Wind farm generation level
$\gamma$	Wind speed level
$f_X(\cdot)$	Probability density function (PDF) of $X$
$F_X(\cdot)$	Cumulative density function (CDF) of $X$
$L_X(\cdot)$	Level crossing rate (LCR) function of $X$
$\mathcal{N}$	Standard normal random variable
$W_{\bar{m}}^{\mathcal{N}}(t)$	Gaussian transformation of $W_{\bar{m}}(t)$
$\phi$	Regression coefficient of the first-order autoregressive (AR(1)) model
$\varepsilon(t)$	White noise of the AR(1) model
$\sigma_\varepsilon$	ariance of $\varepsilon(t)$
$\mathcal{S}$	State space of Markov chain (MC)
$N_s$	Number of states in $\mathcal{S}$
$S_k$	State $k$ in $\mathcal{S}$ , $k \in \{1, \dots, N_s\}$
$\tau_k$	Average duration of state $S_k$
$P_{ag,k}$	Representative generation level of state $S_k$
$Q$	Transition matrix of Markov chain

Table 2.1 (continued)

Notation	Definition
$n_{ij}$	Number of transitions from $S_i$ to $S_j$ encountered in the measurement data
$\Pr(A)$	Probability of an event A
$\mathbb{E}[X Y]$	Conditional expectation of $X$ given $Y$
$\arg \min$	Argument of the minimum

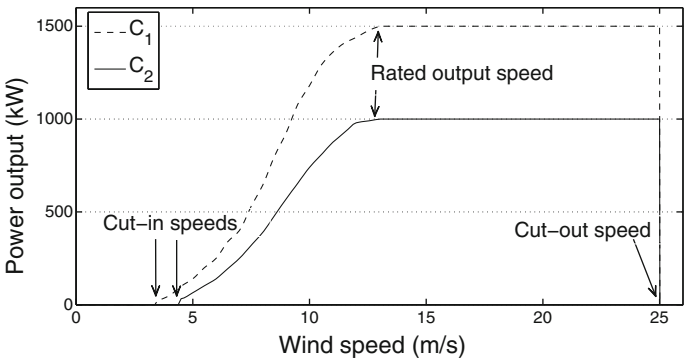


Fig. 2.1 Power curves for wind turbines from classes  $C_1$  and  $C_2$

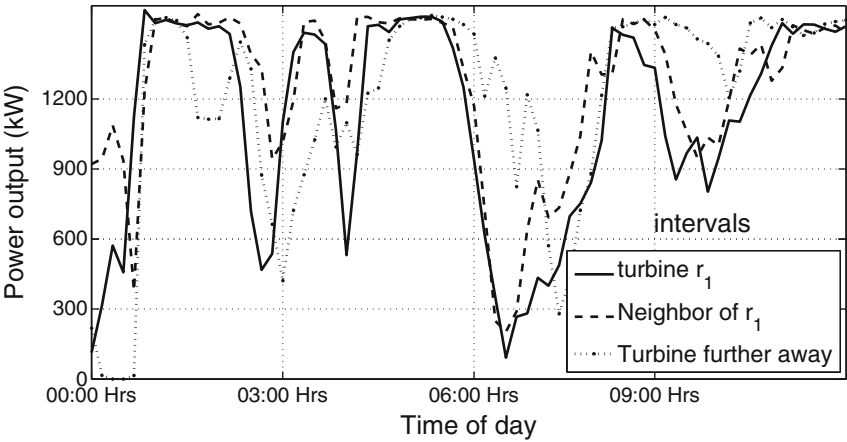
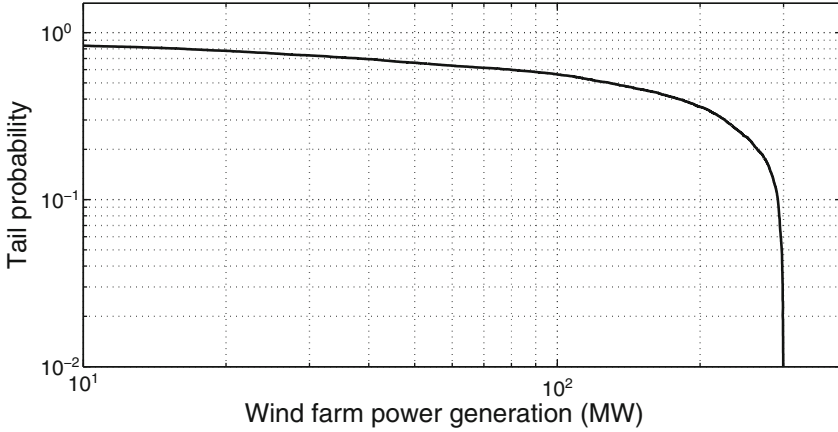


Fig. 2.2 Power outputs of three wind turbines in  $C_1$

outputs of three wind turbines in  $C_1$ . It is clear that the power outputs are not equal, despite the geographic proximity of  $r_1$  and its nearest neighbor (the disparity in the power outputs of the wind turbines belonging to  $C_2$  has also been observed; the plots are not included for the sake of brevity). This disparity has been largely neglected in the existing literature.

Although the variable power outputs of wind turbines are not identical, it is reasonable to assume that they follow the same probability distribution if the wind



**Fig. 2.3** Tail probability of the wind farm's aggregate power output

turbines are of the same class. A natural question here is whether the CLT, either the classic CLT or the generalized CLT, can be applied to characterize the probability distribution of the aggregate power output of a large number of wind turbines. To this end, the tail probability distribution of the wind farm's aggregate power output is examined and plotted in Fig. 2.3. As illustrated in Fig. 2.3, the tail probability demonstrates a “power-law” decay with an exponential cut-off and the power-law part has a much heavier tail than the Gaussian distribution. It is useful to note that this kind of tail behavior has been observed in many natural phenomena (e.g., size of forest fires) that have strong component-wise correlations [19]. Because of the strong correlation between the power outputs of wind turbines, particularly from adjacent wind turbines, the classic CLT cannot be applied to characterize the probability distribution of the wind farm's aggregate power output. In fact, even the “CLT under weak dependence” cannot be directly applied, despite the fact that the correlation between the power outputs of wind turbines weakens with the distance between them (the “mixing distance”). Hence, the probability distribution of the wind farm's aggregate power output cannot be characterized using the classic CLT; and it may not even be governed by stable laws [26]. With this insight, the proposed approach resorts to graphical learning methods to model the dependence structure in the power outputs of individual wind turbines and carries out spatio-temporal analysis accordingly.

### 2.2.2 Diurnal Non-Stationarity and Seasonality

Another key observation, as illustrated in Fig. 2.4, is the diurnal non-stationarity and the seasonality of wind farm generation. Specifically, it is observed that within each 3-h epoch, the probability distributions of wind farm generation over three consecutive 1-h intervals are consistent. However, these CDFs from different epochs of 3 h

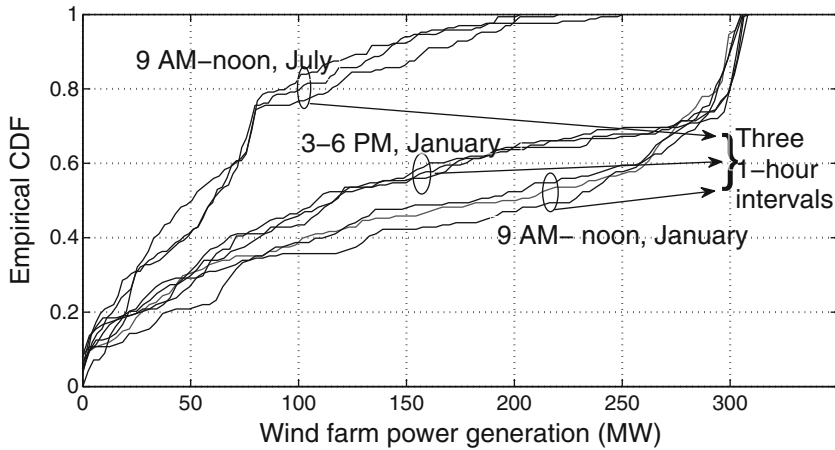


**Fig. 2.4** Empirical distributions of wind farm generation over various 1-h intervals of different epochs of the day and different months

and different seasons can be quite different, indicating the non-stationarity of wind farm generation. Due to the non-stationary (empirical) distributions of wind farm generation, the distributional forecasts and point forecasts of wind farm generation, together with the developed models (Weibull distributions and Markov chains) used to derive distributional forecasts, can have quite different parameters for different months and different epochs. Therefore, it is necessary to develop forecast models *separately* for each month and each epoch (3 h for the wind farm considered here). Further, when estimating the parameters of Weibull distributions and Markov chains, relevant historical data, i.e., the historical data from the same month and the same epoch, can be used.

In what follows, data-driven analysis is carried out to characterize the spatial and temporal dynamics of the wind farm's aggregate power output. The data of the year 2009 is used in spatio-temporal analysis to guide the design of Markov chains, and the data of the year 2010 is used to assess the accuracy of the forecast provided by the proposed Markov-chain-based approach. Specifically, the 9 AM–noon epoch of January 2009 is used as an illustrative example in the following spatio-temporal analysis, since *this epoch exhibits the richest spatio-temporal dynamics, in the sense that the wind farm's aggregate power output during this epoch takes values ranging from 0 to the wind farm's rated capacity and exhibits the highest variability over time (quantified by LCR).*

### 2.2.3 Weibull Distribution of Wind Speed

In the existing literature, wind speed is usually characterized using Weibull distributions [28]. In this work, it is observed from the measurement data that the wind

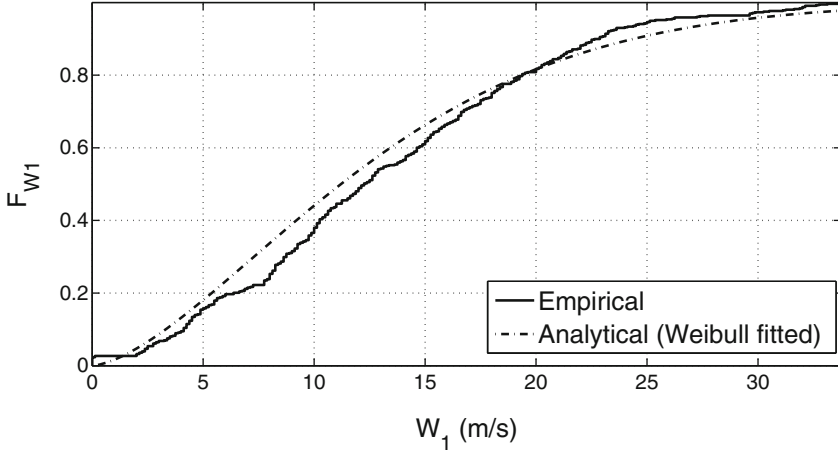


**Fig. 2.5** Weibull-fitted CDF ( $\lambda=11.37$ ,  $k=1.54$ ) and empirical CDF of  $W_1$  for the 9 AM-noon epoch of January 2009

speed  $W_m$  at each MET within the wind farm closely follows a Weibull distribution during each epoch, the probability density function (PDF) of which is given by:

$$f_{W_m}(x) = \frac{k}{\lambda} \left( \frac{x}{\lambda} \right)^{k-1} \exp^{-(x/\lambda)^k}, \quad \forall x \geq 0, \quad (2.1)$$

where  $k$  is the shape parameter and  $\lambda$  is the scale parameter. The fitted cumulative density function (CDF) and the empirical CDF of  $W_1$  for the 9 AM-noon epoch of January 2009 are plotted in Fig. 2.5. The match between the empirical CDF and the fitted CDF suggests that the fitted Weibull distribution with the two parameters  $k$  and  $\lambda$  estimated from wind speed measurements can be utilized to analytically quantify wind speed dynamics. Under the developed spatio-temporal analysis framework, the fitted Weibull distributions of wind speed are also critical to the analytical characterizations of both the statistical distribution and the LCR of wind farm generation. The application of the fitted Weibull distributions of wind speed in the spatial analysis and the temporal analysis will be discussed in Sect. 2.3.1 and 2.3.2, respectively.

## 2.3 Spatio-Temporal Analysis of Wind Farm Generation

### 2.3.1 Spatial Analysis and Statistical Characterization

A key objective of spatial analysis is to characterize the statistical distribution of  $P_{ag}(t)$ . To this end, regression analysis is applied to the measurement data of each turbine's power output, so that  $P_{ag}(t)$  could be expressed in terms of wind speed. Then, the analytical CDF of  $P_{ag}(t)$  can be obtained from the fitted Weibull CDF of wind speed. In what follows, the key steps of spatial analysis are provided in detail.



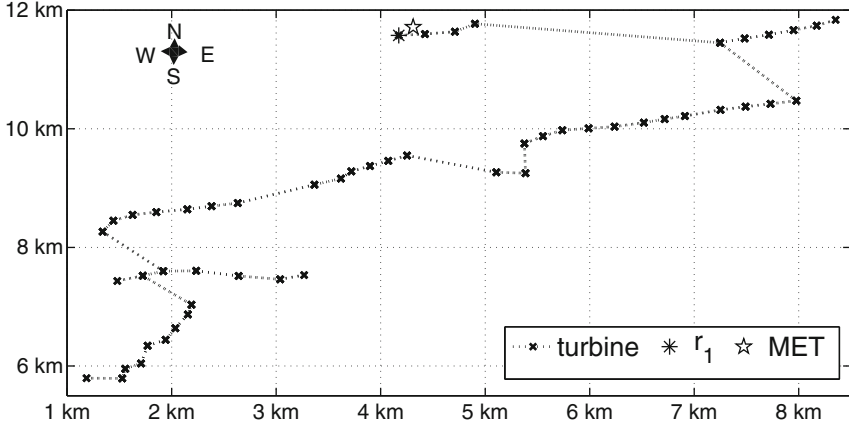


Fig. 2.6 MST of  $C_1$  (with distance to the southwest corner of the wind farm)

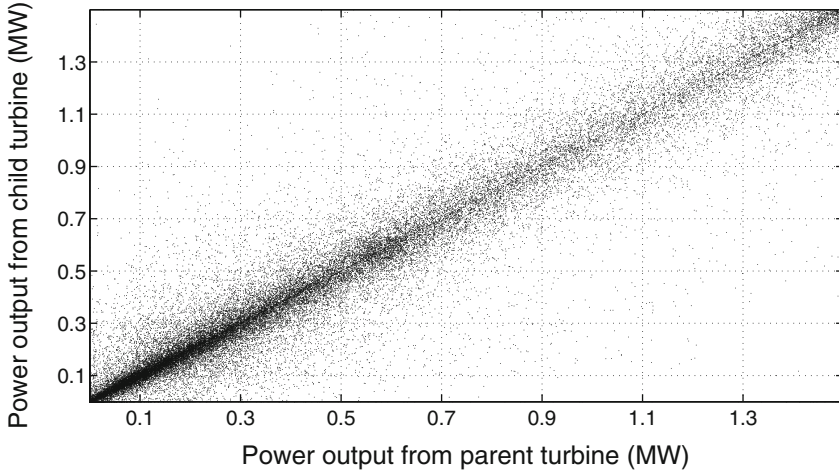


Fig. 2.7 Power outputs of parent-child turbine pairs of  $C_1$  for the 9 AM-noon epoch of January 2009

Using the geographical information of wind turbine locations, a minimal spanning tree (MST) with  $r_m$  as the root node is constructed for each class  $C_m$  by using Prim's algorithm [25], as illustrated in Fig. 2.6. For each wind turbine  $i$  in  $C_m$ , there exists only one path from  $r_m$  to  $i$  in the MST of  $C_m$ . Define the node which is closest to  $i$  along this path as the 'parent' node of  $i$ . Another key observation from the measurement data is that an affine relationship exists between the power outputs of the parent-child turbine pairs for each class, with the case of  $C_1$  illustrated in Fig. 2.7. Therefore, a coefficient  $\alpha_m$  is introduced for  $C_m$ , and the linear regression model  $P_k(t) = \alpha_m P_j(t)$  is used for each parent-child turbine pair  $(j, k)$  in  $C_m$  accordingly.

Further, define  $d_m(i)$  as the number of the nodes (excluding node  $i$ ) along the path from  $r_m$  to node  $i$ , then the linear regression model  $P_i(t) = \alpha_m^{d_m(i)} P_{r_m}(t)$  can be used for any wind turbine  $i$  in  $C_m$ . The value of  $\alpha_m$  is determined by applying the minimum mean square error (MMSE) principle to the aggregate power output of  $C_m$ , as follows:

$$\alpha_m = \arg \min_{\alpha} \frac{1}{N_t} \sum_t \left( P_{ag,m}(t) - \sum_{i \in C_m} \alpha^{d_m(i)} P_{r_m}(t) \right)^2. \quad (2.2)$$

Similarly, an affine relationship between the wind speeds is also observed from the measurement data. For convenience,  $H_1$  is chosen as the reference MET, i.e.,  $\bar{m} = 1$ . Then, the linear regression models for wind speeds are given by  $W_m(t) = \beta_m W_{\bar{m}}(t)$ , where  $\beta_m$  is solved using the MMSE principle as follows:

$$\beta_m = \arg \min_{\beta} \frac{1}{N_t} \sum_t \left( W_m(t) - \beta W_{\bar{m}}(t) \right)^2. \quad (2.3)$$

Using  $P_{r_m}(t) = U_m(W_m(t))$ , the aggregate power output of the wind farm could be characterized as follows:

$$P_{ag}(t) = \sum_m P_{ag,m}(t) = \sum_m \sum_{i \in C_m} \alpha_m^{d_m(i)} U_m(\beta_m W_{\bar{m}}(t)) \triangleq G_{pw}(W_{\bar{m}}(t)). \quad (2.4)$$

Due to the monotone characteristics of  $U_m(\cdot)$ ,  $G_{pw}(\cdot)$  is monotonically increasing. Therefore, the analytical CDF of  $P_{ag}(t)$  can be obtained from the fitted Weibull distribution of  $W_{\bar{m}}(t)$ , given by  $F_{P_{ag}}(\cdot) = F_{W_{\bar{m}}}(G_{pw}^{-1}(\cdot))$ . The analytical CDF and the empirical CDF of  $P_{ag}(t)$  for the considered epoch are illustrated in Fig. 2.8.

It is worth noting that the linear regression models with homogeneous regression coefficients used here are motivated by the observation from the measurement data. The above regression analysis could be generalized by applying more general regression analysis methods. For example, each parent-child turbine pair can have a different linear regression coefficient or the parent-child turbine pairs can be analyzed by using different regression models.

### 2.3.2 Temporal Analysis and LCR Quantification

During each epoch, both the wind speed  $W_{\bar{m}}(t)$  and the wind farm generation  $P_{ag}(t)$  could be regarded as stationary stochastic processes. The LCR of a stochastic process is formally defined as the number of instances per unit time that the stochastic process crosses a level in only the positive/negative direction [29]. Intuitively,  $L_{P_{ag}}(\cdot)$  quantifies how frequently  $P_{ag}(t)$  transits between different generation levels. It will be apparent soon that  $L_{P_{ag}}(\cdot)$ , together with the statistical characterization  $F_{P_{ag}}(\cdot)$ , is critical in designing the state space representation of the Markov chains used for wind farm generation forecast.

Spatio-Temporal Data Analytics for Wind Energy  
Integration

Yang, L.; He, M.; Zhang, J.; Vittal, V.

2014, VIII, 80 p. 34 illus., Softcover

ISBN: 978-3-319-12318-9